Tellus (1987), *39A*, 179–186

Another look at CISK in polar oceanic air masses

By BIN WANG,* *Geophysical Fluid Dynamics Program, Princeton University, Princeton, NJ 08542, USA*

(Manuscript received 17 June; in final form 10 November 1986)

ABSTRACT

Some further theoretical results concerning conditional instability of the second kind (CISK) are derived from Bratseth's model and verified for a more general non-Boussinesq model with a z-dependent heating function. In particular, the minimum threshold moisture content required for the instability, is shown to depend only upon environmental stratification and the vertical distribution of latent heat, while the preferred marginally unstable wavelength, in addition to being dependent on the stratification and the heating distribution, is also proportional to the inverse of the Coriolis parameter. A CISK index, which is defined as the ratio of a characteristic boundary layer specific humidity to the minimum threshold specific humidity of CISK, is used for assessing the relative potential for the CISK development in the Atlantic and the Pacific polar oceanic air masses, compared with that in a tropical oceanic air mass.

The limitation arising from use of a constant heating profile in the interpretation of the short wave cut-off is demonstrated. The criterion for short wave blow-up is analogous to that of convective instability. The necessary and sufficient condition for the presence of short wave cut-off and wave selection is that the threshold moisture content at the shortest wave exceeds the minimum threshold moisture content. The treatment of the unconditional heating intensity is also discussed.

1. The minimum threshold moisture content and preferred marginally unstable wavelength

In his paper (Bratseth, 1985; henceforth referred to as B85), Bratseth derived a formula for CISK growth rate in terms of a Boussinesq model with a constant heating distribution. The growth rate is given by (9) of B85, i.e.,

$$\sigma = DNK\left[\frac{M^2}{N^2}(e^{-\mu H_1} - e^{-\mu H_2}) - 1\right], \tag{1.1}$$

where

$$\mu = NK/f, \tag{1.1a}$$

$$M^2 = \gamma q_s g L \rho_s/[C_p T_0 \bar{\rho}(H_2 - H_1)]. \tag{1.1b}$$

To facilitate reference to B85, the same notations will be used, except the factor γ that has different meaning from that used in B85, as will be discussed shortly in Section 3.

Although the model is an idealized one, the growth rate given by (1.1) depends at least upon the following variables: (1) the strength of the Ekman layer viscosity, D; (2) the buoyancy frequency, N; (3) the Coriolis parameter f; (4) the specific humidity of boundary layer, q_s; (5) the vertical distribution of latent heating, e.g., H_1 and H_2; (6) total horizontal wavenumber, K; (7) the mean density of cloud layer, $\bar{\rho}$; (8) the heating intensity factor γ. This complexity does not invite further analytical, mechanistic analysis and leads to direct calculation in B85.

It seems that, however, some interesting results can be inferred from (1.1), if one examines the instability threshold for CISK. In general, the amplification of a CISK disturbance requires that the moisture content in the boundary layer, say γq_s in B85 (since the effect of changing γ is equivalent to a change in q_s, we consider here their product as one parameter), exceeds a critical

* Present affiliation: Department of Meteorology, University of Hawaii, Honolulu, HI 96822, USA.

value, $(\gamma q_s)_c$, which can be derived directly from (1.1):

$$(\gamma q_s)_c = \frac{C_p T_0 H N^2}{gL} \cdot \frac{(e^{-H_1/H} - e^{-H_2/H})}{(e^{-\mu H_1} - e^{-\mu H_2})}. \quad (1.2)$$

Hereafter this critical value, $(\gamma q_s)_c$, will be referred to as threshold moisture content. In derivation of (1.2) the basic state density is assumed to be $\rho_0(z) = \rho_s e^{-z/H}$, so that $\rho_s/\bar{\rho} = (H_2 - H_1)/H(e^{-H_1/H} - e^{-H_2/H})$, where H is a constant density scale height, $H = RT_0/g$. Note that the threshold moisture content, (1.2), is independent of the turbulent viscosity of the boundary layer. Based upon (1.2), one can further prove the existence of a unique minimum threshold at a particular wavenumber. When $H_1 \neq 0$, the resulting *minimum threshold moisture content*, designated by $\min(\gamma q_s)_c$, is

$$\min(\gamma q_s)_c = \left[\frac{C_p T_0 H}{gL}\right] N^2 \frac{H_2}{H_2 - H_1} \times (e^{-H_1/H} - e^{-H_2/H}) \times \left(\frac{H_2}{H_1}\right)^{H_1/(H_2 - H_1)}, \quad (1.3)$$

which occurs at the total horizontal wavenumber

$$K_p = \frac{f}{N} \frac{\ln(H_2/H_1)}{(H_2 - H_1)}. \quad (1.4)$$

The quantity K_p will be referred to as *preferred marginally unstable wavenumber* and its corresponding x-wavelength as *preferred marginally unstable wavelength*. When the boundary layer moisture content increases and reaches $\min(\gamma q_s)_c$, the wave with preferred marginally unstable wavelength will *first* become unstable. In this sense, the quantity $\min(\gamma q_s)_c$ may be regarded as the minimum moisture content required for any growing CISK mode. As the boundary layer moisture content increases further from the minimum threshold value, the wavelength of the most unstable mode shifts gradually toward the short wave side of the preferred marginally unstable wavelength (Fig. 3 of Wang, 1987).

Several interesting features are observed from (1.3) and (1.4).

(1) The earth's rotation does not affect $\min(\gamma q_s)_c$, implying that the minimum threshold moisture content does not vary with geographic latitude. However, the preferred marginally unstable wavelength decreases with increasing latitude. Taking an example, the ratio of selected marginally unstable wavelength at 15° N (tropical cyclone region) to that of 60° N (polar low region) is about 3.2.

(2) The quantities $\min(\gamma q_s)_c$ and K_p are, respectively, a quadratic and an inverse linear function in the buoyancy frequency, N, indicating the fundamental influences of the environmental stratification on CISK. If N decreases from a typical tropospheric value of 1.1×10^{-2} s^{-1} to 0.7×10^{-2} s^{-1} as used in Fig. 2 of B85, the minimum threshold decreases by 58% and the preferred marginally unstable wavelength reduces by 36%.

(3) The quantities $\min(\gamma q_s)_c$ and K_p respond *sensitively* to the heating parameters H_1 and H_2. Fig. 1 shows that both the minimum threshold moisture content and the preferred marginally unstable wavelength increase rapidly with increasing cloud base, H_1, and cloud thickness, $H_2 - H_1$.

(4) Under *normal* tropospheric conditions, the square bracket quantity in (1.3) does not vary significantly, thus, the minimum threshold moisture content is mainly determined by the stratification and the vertical heating distribution that is closely related to the vertical distributions of temperature and moisture in the environment, in other words, the minimum threshold moisture content depends only upon the thermal structure of an air mass.

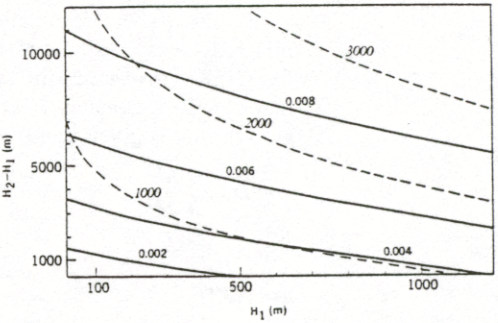

Fig. 1. Contour plot showing the minimum threshold specific humidity, $\min(\gamma q_{sc})$, (solid curves), and the preferred marginally unstable wavelength in units of km (dashed curves) as functions of cloud base H_1 (m) and cloud thickness, $H_2 - H_1$ (m). The other parameters used in the calculations are $N = 0.011$ s^{-1}, $f = 0.000123$ s^{-1}, $T_0 = 270$ K.

Although (1.3) and (1.4) are derived from a Boussinesq model with a constant heating function, it has been verified that the preceding characteristics remain valid qualitatively for a more general non-Boussinesq model with a z-dependent heating profile.

2. The criterion for the short-wave cut-off

The problem of short wave cut-off associated with the important wave selection mechanism has been a major concern in the CISK theories. The interpretation offered in B85 was based on the vertical decay scale of the response, $\lambda f/N$, where λ is horizontal wavelength. It was suggested that the reason for the losing of "short wave cut-off" in case IIa (Fig. 2 of B85) is that the heating reaches the top of the boundary layer, namely, $H_1 = 0$. However, according to solution (1.1), for $H_1 = 0$, the growth rate

$$\sigma \to DNK\left(\frac{M^2}{N^2} - 1\right), \quad \text{as } k \to \infty, \tag{2.1}$$

indicating that, when $M^2 < N^2$, the short waves remain stable, even if the influence of the heat source reaches the boundary layer. The growth rate increases monotonically with decreasing wavelength, i.e., short waves blow up, only when

$$M^2 > N^2. \tag{2.2}$$

In case IIa of Fig. 2 in B85, criterion (2.2) is indeed satisfied.

As far as the short wave cut-off is concerned, the result derived from a model with a constant heating profile may be quite misleading. For instance, when $H_1 = 0$, the threshold moisture content (1.2) reduces to

$$(\gamma q_s)_c = \frac{C_p T_0 H N^2}{gL} \frac{(1 - e^{-H_2/H})}{1 - e^{-\mu H_2}}, \tag{2.3}$$

which is a monotonically decreasing function of K, namely, the shortest wave is the preferred marginally unstable wave. Since (2.2) serves also as an instability criterion for the shortest wave, there is no short wave cut-off, even if $M^2 < N^2$. In what follows, it will be shown that this result is not valid for a model with a more general heating profile.

Let us replace the constant heating profile by a general z-dependent heating profile in the model of B85, write

$$\overline{Q} = \frac{\gamma q_s L \rho_s}{\overline{\rho}(H_2 - H_1)} \eta(z)\, w_s, \tag{2.4}$$

where the vertical integration of $\eta(z)$ from H_1 to H_2 is required to be $H_2 - H_1$. The corresponding eigenvalue problem for the instability becomes (see (3), (5), and (6) of B85)

$$\frac{d^2 W}{dz^2} - \mu^2 W = -\frac{M^2}{f^2} K^2 W_s \eta(z), \tag{2.5a}$$

$$W \to 0, \quad \text{as } z \to \infty, \tag{2.5b}$$

$$\sigma W = Df \frac{dW}{dz}, \quad \text{at } z = 0, \tag{2.5c}$$

where $W(z) = \tilde{w}(z,t)\, e^{-\sigma t}$, $W_s = W(0)$, and μ and M^2 are defined by (1.1a,b). A solution satisfying the upper boundary condition (2.5b) and the matching conditions at $z = H_2$ (i.e., W and dW/dz are continuous) is

$$W(z) = \begin{cases} A e^{-\mu z}, & z \geqslant H_2, \\ e^{\mu z} \displaystyle\int_z^{H_2} \frac{M^2}{2N^2} W_s \mu e^{-\mu t} \eta(t)\, dt \\ \quad + e^{-\mu z}\left[\displaystyle\int_{H_2}^{z} \frac{M^2}{2N^2} W_s \mu e^{\mu t} \eta(t)\, dt + A\right], \\ \quad H_1 \leqslant z \leqslant H_2, \\ B e^{\mu z} + (W_s - B) e^{-\mu z}, \quad 0 \leqslant z \leqslant H_1, \end{cases} \tag{2.6}$$

Using the condition that $W(z)$ is continuous at $z = H_1$ and the lower boundary condition (2.5c), we obtain the growth rate

$$\sigma = \frac{DK}{N}\left[\int_{H_1}^{H_2} M^2 \mu \eta(z) e^{-\mu z}\, dz - N^2\right], \tag{2.7}$$

and the threshold moisture content

$$(\gamma q_s)_c = \frac{C_p T_0 N^2 H (e^{-H_1/H} - e^{-H_2/H})}{gL \displaystyle\int_{H_1}^{H_2} \mu \eta(z) e^{-\mu z}\, dz}, \tag{2.8}$$

where (1.1b) and

$$\rho_s/\overline{\rho} = (H_2 - H_1)/H(e^{-H_1/H} - e^{-H_2/H})$$

have been used. In the limit of $K \to \infty$, the growth rate

$$\sigma = \frac{DK}{N}[M^2 \eta(0) - N^2], \tag{2.9}$$

which indicates that the instability behavior at the shortest wavelength is determined by the competitive effect between the latent heat

released *in situ* at the top of the boundary layer (the first term on the r.h.s.) and the Ekman pumping-induced cooling (the second term on the r.h.s.), rather than determined just by the amount of heating released within the vertical decay scale of the shortest wave. Eq. (2.9) shows that, when the cloud base is located above the boundary layer (hence $\eta(0) = 0$), short waves are stable; however, when the latent heating reaches the boundary layer and

$$M^2\eta(0) - N^2 > 0, \tag{2.10a}$$

the short waves blow up. This agrees with the result derived by Pedersen and Rasmussen (1985). It is interesting to notice that the criterion for short wave blow-up, (2.10a), is the same as the instability criterion for the shortest wave:

$$\gamma q_s > \frac{C_p T_0 N^2 H(1 - e^{-H_1/H})}{gL\eta(0)} = (\gamma q_s)_c|_{K\to\infty}. \tag{2.10b}$$

We now focus on the problem of the short wave cut-off. We note that

$$M^2\eta(0) - N^2 \leqslant 0, \quad \text{or } \gamma q_s \leqslant (\gamma q_s)_c|_{K\to\infty} \tag{2.11}$$

is only one of the necessary conditions for the short wave cut-off. The presence of short wave cut-off also requires that the preferred marginally unstable wave occurs in the middle-wavelength. Thus the short wave cut-off crucially depends upon the characteristics of the instability threshold $(\gamma q_s)_c$ as a function of the wavenumber. In terms of the moisture content of the boundary layer, a necessary and sufficient condition for the short wave cut-off may be written as

$$\min(\gamma q_s)_c < \gamma q_s \leqslant (\gamma q_s)_c|_{K\to\infty}. \tag{2.12}$$

In the case of constant heating profile (see (2.3)), $\min(\gamma q_s)_c = (\gamma q_s)_c|_{K\to\infty}$, the short-wave cut-off is missing. To demonstrate this is not valid for a z-dependent heating profile, we specify a sinusoidal heating profile

$$\eta(z) = A \sin a(z - H_0), \tag{2.13a}$$

$$A = \frac{a(H_2 - H_1)}{1 + \cos a(H_1 - H_0)}, \quad a \equiv \frac{\pi}{H_2 - H_0}, \tag{2.13b}$$

where H_0 is a parameter that allows heating to occur at H_1, if $H_1 > H_0$. When heating takes place at the top of the boundary layer, i.e., $H_1 = 0$ and $H_0 < 0$, the threshold moisture content (2.8) becomes

$$(\gamma q_s)_c = \frac{C_p T_0 HN^2}{gLAH_2} \times \frac{(\mu^2 + a^2)(1 - e^{-H_1/H})}{\mu[a(\cos aH_0 + e^{-\mu H_1}) - \mu \sin aH_0]}. \tag{2.14}$$

To facilitate comparison, the threshold specific humidities (2.14) and (2.3) are plotted by solid and dashed curves, respectively, in Fig. 2. In the presence of a sinusoidal heating profile, the preferred marginally unstable wave occurs at a middle-wavelength, thus, the short wave cut-off exists as long as the condition (2.12) is satisfied. The qualitative difference between (2.3) and (2.14) reveals the limitation resulting from the use of a constant heating profile in interpreting the short wave cut-off.

It has been shown in this section that the criterion for short wave blow-up (2.10a), is equivalent to the instability criterion at the shortest wave (2.10b). Both of them indicate that, if the effect of the latent heating *in situ* at the top of the boundary layer predominates over that of the Ekman pumping-induced cooling, the short waves blow up. They also imply that the effective static stability at the top of the boundary layer is negative, a condition analogous to that of convective instability. In fact, the short wave blow-up simply means the break-down of the

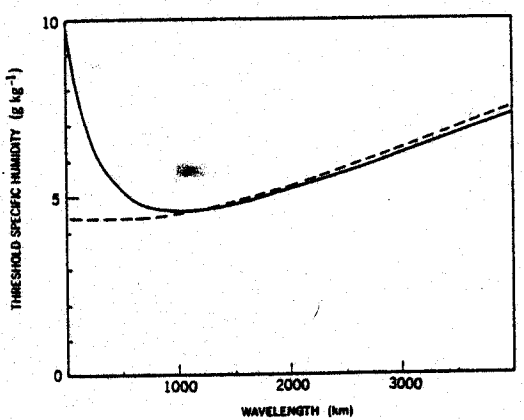

Fig. 2. The threshold specific humidity calculated using a sinusoidal heating function (solid curve) and using a constant heating function (dashed curve) as functions of wavelength. The parameters used in (2.14) and (2.3) are $N = 0.011\ s^{-1}$, $f = 0.000123\ s^{-1}$, $T_0 = 265$ K, $H_2 = 4500$ m, $H_1 = 0$ m, $H_0 = -500$ m.

basic assumption of CISK and the onset of convective instability.

The presence of the short wave cut-off, on the other hand, is shown to be characterized by a finite preferred marginally unstable wavelength; the latter quantity is in turn determined by the integral property of the vertical heating distribution, the stratification and the planetary vorticity as implied by (2.8). A necessary and sufficient condition for the presence of the short wave cut-off and wave selection is that the minimum threshold moisture content must be less than the threshold moisture content at the shortest wave.

3. The intensity factor γ in the unconditional heating representation

Arguing that there is a possible overestimation in CISK growth rate by using unconditional heating, Bratseth (1985) introduced an intensity factor γ in his representation of heating strength. A simple truncated Fourier decomposition of $\cos(x)$ to the sum of a constant component, π^{-1}, and a wave component, $\frac{1}{2}\cos(x)$ (Fig. 1 of B85), leads to his choice of $\gamma = 0.5$, because a constant heating component has no contribution to development of CISK disturbance in a *linear* analysis. However, the conditional heating is essentially nonlinear. Neglecting the effect of the constant heating component is not justified in a *nonlinear* response of instability to convective heating, simply because the interaction between the modes induced by two heating components may have nonnegligible contribution to the instability.

One of the possible approaches to assess the consequence of using the unconditional heating representation may be to examine the differences in behavior of a system under conditional and unconditional heatings. This has been undertaken by Syono and Yamasaki (1966) and by Koss (1975). Syono and Yamasaki (1966) reported that, for hurricane-scale disturbance, the upward and downward motions calculated using an unconditional heating had a nearly equally spaced symmetric distribution, whereas in the case of conditional heating, strong upward motion was concentrated in a relatively narrow region, while weak downward motion spreads over a wider region in an interval of one wavelength. No overestimation in the growth rate by using unconditional heating was reported for this mode. On the basis of the results from his numerical integration, Koss (1975) concluded that the derived instability diagram for conditional heating case is remarkably similar to that of the comparable unconditional heating case, except for a shift of the preferred wavelength interval toward longer wavelengths. In a recent numerical study, P. R. Bannon also found that use of a conditional heating leads to a development almost as strong as the unconditional case but the wavelength of the disturbance is longer under the conditional heating (personal communication). These numerical experiments do not verify the rationality of the choice of $\gamma = 0.5$ by neglecting the constant heating components.

On the other hand, in the parameterization of cumulus heating, (4) of B85, it was implicitly assumed that the moisture that converges into an air column through the top of boundary layer is completely condensed out and all the latent heat released in cloud is absorbed by the air column. Apparently, this assumption leads to overestimation in the amount of latent heating, because a fraction of the total moisture supply stores in the air and increases the humidity of the environment. In view of this, the intensity factor γ may be regarded as a coefficient that measures the ratio of convective precipitation to the total amount of moisture converging into cumulus cloud ensemble, and in reality, the value of γ varies with the environmental moisture distribution and should be less than 1.

4. Possibility of the CISK development in polar oceanic air masses

The CISK has been considered to be a primary mechanism for the development of polar lows (e.g., Rasmussen, 1979). When applying CISK theory to polar lows, we are concerned with the question whether and how a CISK disturbance can grow in polar oceanic air masses. A straightforward approach is to compute the CISK growth rate for parameters relevant to the polar oceanic environment. When so doing, however, one ought to realize that the choice of the value for γ involves uncertainty, besides the CISK

solution is rather sensitive to the intensity and vertical distribution of latent heating and to basic state properties (e.g., the stratification and the latitude). The results derived from an idealized model with particular values of the parameters appear to be inconvincible. On the other hand, as shown in Section 1, use of such a mechanistic model indeed gives a sensible picture of the dependence of CISK growth on its embedded environment. Especially, the minimum threshold moisture content of CISK, depends mainly upon the stratification and vertical heating profile. For a given observed environment, we may first calculate the model-predicted minimum threshold moisture content, then define a CISK index as the ratio of the observed specific humidity (typical to this environment) to the predicted minimum threshold specific humidity. This index should qualitatively reflect the potential for a CISK disturbance to amplify in the environment. By comparing CISK indices, we can, at least to some extent, assess the *relative possibility of the CISK development in polar oceanic air masses, compared with that in tropical oceanic air masses.*

Some tropical CISK models adopted a balance assumption for disturbances with symmetric cylindrical geometry (e.g., Charney and Eliassen, 1964). The resulting eigenvalue problem for instability is the same as that derived from the quasi-geostrophic model here (e.g., Davies and de Guzman, 1979). Since the planetary vorticity is weak in the tropics, a valid balance assumption requires that the pre-existing disturbance has sufficiently strong relative vorticity, and this is one of the weaknesses of the tropical CISK (Ooyama, 1982). Nevertheless, the quasi-balanced CISK modes are still justifiable even in a primitive equation model (Syono and Yamasaki, 1966). In the tropics, cumulus convection often penetrates a much deeper conditionally unstable tropospheric layer than in polar ocean region where the tropopause is substantially lower than in the tropics. To obtain a better estimation, a non-Boussinesq model is desirable.

It is shown that for a non-Boussinesq model with constant density scale height, H, and buoyancy frequency, N, the threshold moisture content for CISK is

$$(\gamma q_s)_c = \frac{C_p T_0 H f^2 r_1}{gLK^2} \frac{(e^{-H_1/H} - e^{-H_2/H})}{\int_{H_1}^{H_2} \eta(z) e^{-r_1 z} dz}, \quad (4.1)$$

where

$$r_1 = [N^2 K^2/f^2 + 1/(4H^2)]^{1/2} + 1/(2H). \quad (4.2)$$

In the case of constant heating, $\eta(z) = 1$, (4.1) reduces to

$$(\gamma q_s)_c = \frac{C_p T_0 H f^2 r_1^2}{gLK^2} \frac{(e^{-H_1/H} - e^{-H_2/H})}{(e^{-r_1 H_1} - e^{-r_1 H_2})}. \quad (4.3)$$

When the density scale height H approaches infinity, (4.3) recovers the result for a Boussinesq model (1.2).

Table 1 summarizes the minimum CISK threshold specific humidity (when $\gamma = 1$), the preferred marginally unstable wavelength and the CISK indices computed using (4.3) for five different cases. Parameters in Case I are assumed to be relevant to a tropical environment located at

Table 1. *The minimum CISK threshold specific humidity, preferred marginally unstable wavelength and CISK index for tropical, Atlantic, and Pacific polar air masses; in all cases, the height of cloud base, H_1, is assumed to be 500 m and the heating intensity factor γ to be 1*

Cases	f (10^{-4} s^{-1})	N (10^{-2} s^{-1})	H_2 (m)	Minimum threshold specific humidity (g kg^{-1})	Preferred marginally unstable wavelength (km)	CISK index
I Tropical	0.38	1.1	12,000	9.3	8,000	1.72
II Comparison	1.23	1.1	12,000	9.3	2,500	
III Comparison	1.23	1.1	4,000	5.4	1,350	
IV Atlantic Polar	1.23	1.0	4,000	4.5	1,200	1.11
V Pacific Polar	1.23	1.0	5,500	5.3	1,450	0.94

15°N. Cases II and III are just for comparisons. Case IV represents a typical Atlantic polar oceanic environment where the buoyancy frequency takes a smaller value of 10^{-2} s^{-1}; this value corresponds to the conditions over the stable layer on the Bear Island sounding from 12.00 GMT December 12, 1982 shown as Fig. 9 in Rasmussen (1985). The parameters in the last case are assumed to fit Pacific polar lows, where the cloud top is often higher than that in the Atlantic polar lows. The choice of cloud height H_2 for both Atlantic and Pacific polar lows are based upon the heating profiles of Sardie and Warner (1985), which are obtained from the Fritsch/Chappel and Anthes cloud models using soundings of temperature and dewpoint that are representative of the Atlantic and Pacific polar lows. In the calculation of CISK index, the characteristic values of boundary layer specific humidity are assumed to be 16 g/kg for tropical air masses and 5 g/kg for polar oceanic air masses, respectively. For the rest of the parameters, the following common values are used: $C_p = 1004$ m^2 s^{-2} K^{-1}, $T_0 = 265$ K, $L = 2.5 \times 10^6$ m^2 s^{-2}, $R = 287$ m^2 s^{-2} K^{-1}, $g = 9.8$ m s^{-2}, $K^2 = 2$ k^2, and $H_1 = 500$ m.

Comparison of case II with case I confirms that change of latitude from 15°N to 60°N does not affect the minimum threshold moisture content but reduces the preferred marginally unstable wavelength remarkably. In comparison with case II, case III exhibits the effect of decreasing cloud thickness. Note that, when the cloud thickness decreases from 11,500 m to 3500 m (decreases by 70%), the minimum threshold moisture content reduces from 9.3 g kg^{-1} to 5.4 g kg^{-1} (decreases by only 54%). As compared with case III, case IV shows the important effect of reduced stratification on the growth of CISK disturbances. It is seen from Table 1 that the CISK indices for polar oceanic air masses, especially in the Pacific polar oceanic region, are considerably lower than that for tropical air masses, suggesting that the potential for a growing CISK mode occurring in polar oceanic air masses is appreciably smaller than that in tropical oceanic air masses.

It should be pointed out that, in principal, one can use more realistic vertical heating distribution functions suited for the tropical oceanic and polar oceanic air masses and the generalized formula (4.1) to make a better estimation of the minimum threshold moisture content and the CISK index. The results given in Table 1 have included the most significant difference of the heating profile between the tropical and polar oceanic air masses, namely, the different height of the cloud top. The conclusion is, therefore, expected to be qualitatively robust. It is also clear from Table 1 that the potential for CISK development in polar air masses increases with (1) decreasing stratification of the environment, and/or (2) decreasing vertical extent of the convective cloud layer. Over polar ocean region, extremely strong flux of surface sensible heat contributes to the reduction of static stability, thus may effectively enhance the instability. In general, however, since the polar oceanic environment is less favorable for CISK than tropical oceanic environment, it is suggested that other physical processes may play important roles on the rapid growth of the polar lows. Baroclinic forcing associated with polar front may contribute to the combined baroclinic-CISK instability as demonstrated by theoretical analyses of Mak (1982) and Wang and Barcilon (1986), and by numerical experiments of Sardie and Warner (1985) and Orlanski (1986).

5. Acknowledgements

I would like to thank Drs. I. Held, F. B. Lipps and J. Mahlman for reading the manuscript and for the helpful discussions. The comments on an earlier version of the manuscript by Dr. Bratseth are helpful in clarifying the text. My thanks also go to Mrs. J. Callan for typing the manuscript. This work was supported by the NOAA/Princeton University grant NA84EAD00057.

REFERENCES

Bratseth, A. M. 1985. A note on CISK in polar air masses. *Tellus 37A*, 403–406. Polar Low Special Issue.

Charney, J. G. and Eliassen, A. 1964. On the growth of the hurricane depression. *J. Atmos. Sci. 21*, 68–75.

Davies, H. C. and de Guzman, R. A. 1979. On the preferred mode of Ekman-CISK. *Tellus 31*, 406–412.

Koss, W. J. 1975. Linear stability analysis of CISK-induced low latitude disturbances. NOAA Tech. Memo. ERL WMPO-24, 176 pp. [NTIS No. PB248 450.]

Mak, M. 1982. On moist quasi-geostrophic baroclinic instability. *J. Atmos. Sci. 39*, 2028–2037.

Orlanski, I. 1986. Localized baroclinicity: a source for meso-α cyclones. *J. Atmos. Sci. 43*, (December) in press.

Ooyama, K. 1982. Conceptual evolution of the theory and modeling of the tropical cyclone. *J. Meteorol. Soc. Japan 60*, 369–379.

Pedersen, T. S. and Rasmussen, E. 1985. On the cut-off problem in linear CISK-models. *Tellus 37A*, 394–402. Polar Low Special Issue.

Rasmussen, E. 1979. The polar low as an extratropical CISK disturbance. *Q. J. R. Meteorol. Soc. 105*, 531–549.

Rasmussen, E. 1985. A case study of a polar low development over the Barents Sea. *Tellus 37A*, 407–418. Polar Low Special Issue.

Sardie, J. M. and Warner, T. T. 1985. A numerical study of the development mechanisms for polar lows. *Tellus 37A*, 460–477. Polar Low Special Issue.

Syono, S. and Yamasaki, M. 1966. Stability of symmetrical motions driven by latent heat release by cumulus convection under the existence of surface friction. *J. Meteorol. Soc. Japan 44*, 353–375.

Wang, B. 1987. The nature of CISK in a generalized continuous model. *J. Atmos. Sci. 44*, (April) in press.

Wang, B. and Barcilon, A. 1986. On the moist stability of a baroclinic zonal flow with conditionally unstable stratification. *J. Atmos. Sci. 43*, 705–719.